Accepted for presentation in: IEEE Future Networks World Forum (FNWF), Bangalore, India, November 2025.

6G Network Design with Custom-tailored IRSs for Sustainable Millimeter-wave Connectivity Enhancements in Industrial Environments

Simon Häger, Melina Geis, Kevin-Ismet Šabanović, Pascal Jörke, Stefan Böcker, and Christian Wietfeld
Communication Networks Institute (CNI), TU Dortmund University, 44227 Dortmund, NRW, Germany
E-mail: {Simon.Haeger, Melina.Geis, Kevin.Sabanovic, Pascal.Joerke, Stefan.Boecker, Christian.Wietfeld}@tu-dortmund.de

***Abstract*—Private millimeter-wave (mmWave) networks offer immense potential for indoor factory (InF) environments by enabling ultra-high data rates and network capacity to support advanced industrial applications. However, their performance is significantly challenged in non-line-of-sight (NLOS) situations, where severe attenuation may lead to insufficient connectivity. Traditionally, this limitation requires the deployment of additional base stations (BSs), which increases both the costs and energy consumption. To address these challenges efficiently, future 6G networks will leverage intelligent reflecting surfaces (IRSs) to illuminate under-connected regions. The passive-static *HELIOS* IRS concept has reached a high maturity level compared to other solutions, with field experiments successfully demonstrating its ability to enhance various link metrics in predetermined regions. This work now investigates how to systematically determine the required number of IRSs, their placement, and preconfigured reflection characteristics. Our proposed brownfield network planning scheme for IRSs thereby takes an important step toward solving the open research problem of 6G hybrid network planning. Using a real-world production scenario from previous measurement campaigns, we demonstrate that one BS with three custom-tailored passive IRSs eliminates the need for a second active BSs while maintaining the required service quality level.**

***Index Terms*—6G network planning, mmWave communication, static-passive IRS, indoor factory, ray-tracing, reflection model.**

I. Toward Industry mmWave Networks with IRSs

Wireless communications at mmWave frequencies promise performance improvements by leveraging broad bandwidths. However, the increasingly hostile propagation characteristics of mmWaves compared to the sub-6 GHz spectrum, particularly regarding object penetration capabilities, pose challenges for widespread deployment in urban and indoor environments [1]. Developing such large-scale networks would be costly, as numerous full-blown BSs would be required [2]. This has been a major hurdle to the global adoption of 5G mmWave technology. *Hence, within the sustainability goals of 6G, the effective cell coverage area must be expanded in a cost- and energy-efficient manner while ensuring a high service quality.*

IRSs, mounted at optimal positions with bespoke reflection characteristics, can effectively introduce reflections into under-connected regions near BSs, particularly at locations where users experience NLOS conditions [3]. Considering private cellular networks, IRSs introduce an opportunity to flexibly improve the control over the radio environment, i.e., without relocating, rewiring, and restarting existing BSs or adding costly active BSs, to ensure operational reliability and address specific industrial requirements. This flexibility is crucial because shop floor layouts can be complex and evolve over time [4, 5]. For instance, connectivity is reduced in some regions when a new large machine is set up or overhead cranes move goods [6]. In such cases, it is practical to mount a low-cost, entirely passive reflector at a strategic position on arbitrary factory walls, ceilings, or machines to mitigate the problem. Therefore, this work focuses on identifying the required number of IRSs, as well as their positions and configurations, i.e., we conduct brownfield 6G network planning with IRSs. This topic has been addressed by only a few research works so far [7, 8]. Moreover, it is an important step toward the open 6G research problem of hybrid network planning, which handles both active and passive infrastructure components [9].

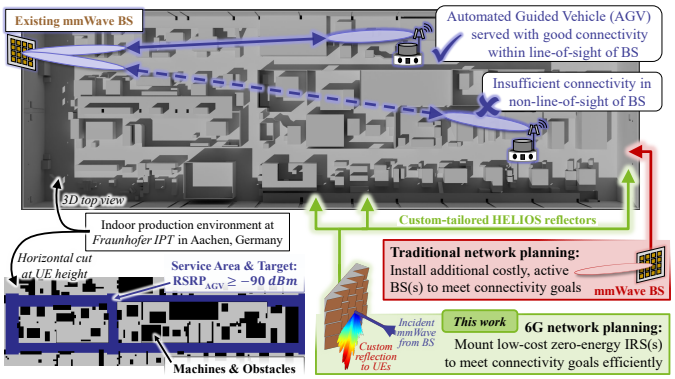

Fig. 1. Private mmWave network connects AGVs for automated production. Traditional brownfield network planning deploys additional full-blown BSs to guarantee the required connectivity level in NLOS regions. This work demonstrates a sustainable 6G alternative: we determine the required number of IRSs, their mounting positions, and custom-design the HELIOS reflectors.

Against this background, Sec. II introduces a complex InF environment featuring a private cellular mmWave network. Considering the targeted service level for mobile AGVs, we first characterize the connectivity levels achieved using one or two BSs. Sec. III presents a hybrid network planning approach designed to efficiently achieve the desired service quality in the target area with only one active BS complemented by zero-power custom-tailored IRSs placed at strategic locations. Finally, Sec. IV summarizes our findings and provides insights into ongoing research on 6G network planning with IRSs.

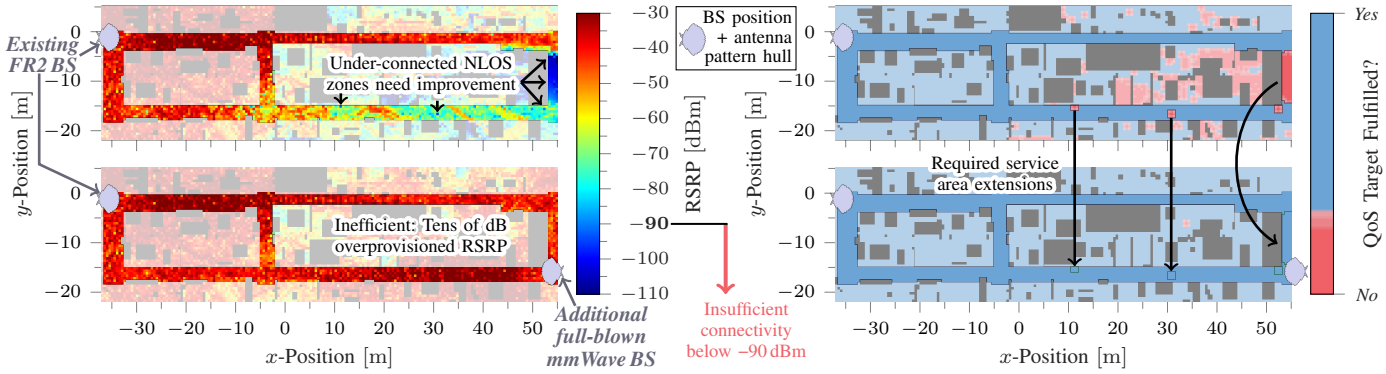

Fig. 2. Traditional network planning addresses under-connected regions by unsustainable deployment of additional active BSs: mmWave connectivity in the production hall is *(top row)* insufficient with single BS but *(bottom row)* drastically over-provisioned with two costly BSs, as illustrated by *(left column)* attained received power level and *(right column)* its classification considering the considered QoS target (RSRP $\geq -90\,\mathrm{dBm}$).

II. mmWave InF Connectivity with BSs

This section first presents the production scenario, network setup, and communication QoS targets in Sec. II-A, before discussing the attained baseline connectivity levels in Sec. II-B.

A. Private Indoor Factory Radio Environment

A real-world large-scale production scenario from *Fraunhofer IPT* [10] in Aachen, Germany is considered in this case study, featuring a shop floor area of more than 2,700 m^2. The factory hall has a length of 97 m, width of 28.5 m, and ceiling height of approximately 10 m, as shown from top view at the top of Fig. 1. More than 50 machine tools and work spaces are used for various production steps. They consist of and are surrounded by metallic components that suppress penetration by electromagnetic (EM) waves. Overall, the scenario matches the 3GPP indoor factory (InF) definition [11, Tab. 7.2-4].

From the application side, this work focuses on the key pathways, i.e., two long (horizontal) and three shorter (vertical) corridors, that are used by AGVs to transport goods between machines and storage [12]. Hence, these 2.0 m to 2.6 m broad transportation lanes, as highlighted in blue at the bottom left corner of Fig. 1, need to be served with a sufficient connectivity of at least 1 Gbit/s [13, Ch. 4.4], i.e., it is aimed for $\geq -90\,\mathrm{dBm}$ RSRP based on experiments in [3].

We consider two network deployments mirroring our previous experimental works: the first setup features a single BS at position $[-37.30\,\mathrm{m}, -1.19\,\mathrm{m}, 6.00\,\mathrm{m}]$, cf. placement in Fig. 1, which is intended to serve the upper long corridor [14]. Our second setup extends the first one by a second BS at the position $[55.55\,\mathrm{m}, -15.87\,\mathrm{m}, 6.00\,\mathrm{m}]$, which is outlined by the red arrow in Fig. 1, to serve the lower long corridor [6]. Both cells are mounted at the height of 6.0 m and operate at the center frequency of 27.1 GHz using 33 dBm transmit power (2 W EIRP). The RSRP is determined using the commercial ray-tracer *Wireless InSite* [15] with the same settings as in the prior EM simulation-complemented field study [14]. In the following sections, we consider the simulation results for a 9,936-element rectangular user equipment (UE) position grid with 0.5 m uniform spacing at a height of 1.0 m. The obstacle distribution at this height realizes in a clutter density of 25.05 %.

B. AGV Connectivity Assessment with One and Two BSs

Fig. 2 presents the attained connectivity levels throughout the production hall. The single BS setup in the top row has a strong user connectivity in the line-of-sight (LOS) with RSRP values far above the connectivity targets. However, the attained RSRP values in NLOS modality do not meet the −90 dBm target in an aggregated area of approximately 20 m^2, with a power gap of up to 37.02 dB. Hence, this simple network infrastructure deployment is unsuitable for the desired use case.

Against this background, traditional pre-6G network planning would result in an enhanced network deployment with two active mmWave cells [16], cf. bottom row of Fig. 2. The previously poorly connected NLOS area of the first BS is now mitigated such that only a few positions in the entire production hall do not have sufficient connectivity. While highly suitable from a performance perspective, sustainability aspects are neglected: the costly second BS consumes hundreds of Watts [17, Ch. 5.5] and overprovisions the RSRP inside and outside the targeted service area by tens of decibels (dBs). This stands in contrast to the proclaimed sustainability goals for 6G networks, i.e., delivering high-performance communications while reducing power consumption and network costs. There are numerous mitigation strategies in this context, with this work focusing on the green technology concept of IRSs [18], in particular, fully-passive non-reconfigurable (static) IRSs [3].

III. Meeting Communication Service Requirements Efficiently using Custom-tailored HELIOS Reflectors at Selected IRS Mounting Positions

Considering the previous section, this study aims to extend the single-BS deployment by IRSs in order to efficiently provide the required communication QoS level in the major production corridors compared with using a two-BS setup. For this reason, Sec. III-A introduces an IRS network planning procedure for future 6G networks, including the custom-tailoring step of the Holistic Enlightening of bLackspots with passIve reflectOr moduleS (HELIOS) reflector geometries. The resulting mmWave connectivity is assessed in Sec. III-B with a focus on the QoS compliance after the first and last iterations of the proposed solution approach.

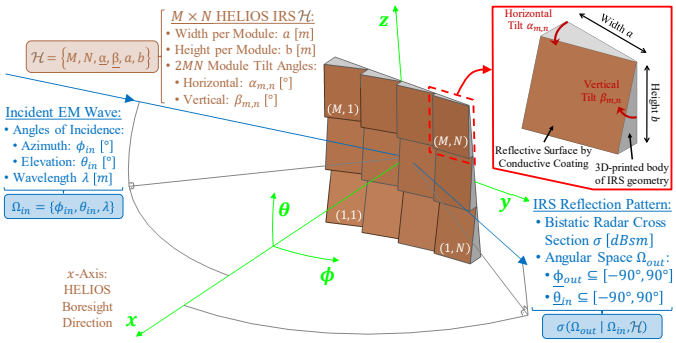

Fig. 3. Overview of employed HELIOS IRS concept for an arbitrary 3×4 geometry $\mathcal{H}$ along with an introduction of its key parameters required for our genetic- and model-based reflection beam shaping [19, 20] leveraged in the scope of this work's network planning process, cf. `Steps #5)` to `#6)`.

A. Proposed Indoor Brownfield Network Planning Approach: How many IRSs? Which Positions and What Configurations?

Whereas traditional network planning aims to guarantee the required service level with the least amount of active communication infrastructure [16], this work instead employs fully passive *HELIOS* reflectors, which are introduced in Fig. 3 and discussed below. By intelligent placement and customization of them, our contribution in this section elevates supposedly simple reflectors to the level of IRSs, which are capable of realizing so-called 6G smart radio environments (SREs).

HELIOS IRSs: Compared to the conventional synthetic approach for IRSs, HELIOS exploits the natural law of reflection with a custom-tailored overall geometry, which results in the desired reflection behavior. To limit the complexity of identifying a suitable geometry, the solution space is reduced to $M \cdot N$ flat surfaces distributed over a uniform $M \times N$ module array. Each module typically has a y-z-plane footprint with width a and height b of several wavelengths λ, respectively, compared to the sub-wavelength unit cell dimensions of conventional metasurfaces. Each reflecting surface (m, n), with $m = 1, \ldots, M$ and $n = 1, \ldots, N$, is tilted horizontally by $\alpha_{m,n}$ and vertically by $\beta_{m,n}$, which are both limited to the angular space $]-90°, 90°[\subseteq \mathbb{R}$. Therefore, it affects the peak reflection direction in the azimuth direction by 2α and elevation direction by 2β, with similar changes for the entire pattern, including sidelobes and nulls. Careful tuning of the tilt angles, module number and dimensions allows for a broad, well-aligned reflection into a targeted service area $\Omega_{out} = \underline{\phi}_{out} \times \underline{\theta}_{out} \subseteq [-90°, 90°]^2$ [19, 20]. For deployment, the geometry is manufactured additively and then coated with a conductive varnish. The potential of such HELIOS IRSs has already been confirmed experimentally, including for a selected production use case wherein the connectivity of an industrial machine within a safety cage was improved [14].

IRS Network Planning Process: Against this background on the considered reflector architecture, we propose an iterative process to scale the IRS deployment to the large service area of the AGVs, as shown in Fig. 4. This is described by the subsequent list of seven steps, as indicated by bullets `1)` to `7)`, along with their key innovations (designated by ➤):

1) Preparatory steps for IRS network planning:
   a) **Baseline connectivity assessment**, cf. Sec. II: Determine RSRP radio environmental map (REM) for active infrastructure deployment and define communication targets in terms of QoS threshold plus service area, with the latter being denoted by UE position set $\mathcal{P}_{UE}$.
   b) Provide **all possible IRS mounting positions** $\mathcal{P}_{IRS}$ in the InF scenario. Here, a set of 4,265 positions with 0.5 m spacing on up to 93 m long surfaces of *(i)* all four walls with heights in the range of 3.5 m to 7.5 m to avoid human and object blockage, and *(ii)* three 1.5 m broad flat patches of suspended ceiling at $z = 8.9$ m.
   c) Consider **IRS design constraints**. Here: Single reflection beam within full hemispheric field of view using a maximum azimuth and elevation reflection beamwidths of 20° for a fixed $50\,\text{cm} \times 50\,\text{cm}$ reflector footprint.
2) **Determine the set of remaining under-connected UE positions $\mathcal{P}_{U-UE} \subseteq \mathcal{P}_{UE}$ in the service area from the overall RSRP REM.** *Terminate if there are none ($\mathcal{P}_{U-UE} = \emptyset$), otherwise initiate s^{th} iteration of our proposed joint HELIOS IRSs placement and configuration process ($|\mathcal{P}_{U-UE}| > 0$).*
   - Considering the baseline connectivity of the single BS, as discussed in Sec. II and shown in the top right subfigure of Fig. 2, `Step #3)` is initiated with $s = 1$.
   - Increment counter s by one when initiating subsequent planning cycles spanning `Steps #3)` to `#6)`.
3) **Identify feasible candidate IRS mounting positions $\mathcal{P}_{C-IRS,s} \subseteq \mathcal{P}_{IRS}$:**
   a) Ignore positions from `Step #1b` that have *(i)* no LOS to the BS or *(ii)* no LOS to at least one under-connected UE position. Determined via ray-tracer.
   b) Further reduce candidate IRS mounting positions to the contained subset of IRS positions that may serve the maximum number of under-connected UE positions $\mathcal{P}_{U-UE,s} \subseteq \mathcal{P}_{U-UE}$.
   c) Also remove candidate IRS positions that are incompatible with IRS design constraints, cf. `Step #1c)`.
4) **Heuristic selection of single IRS mounting position** $\underline{p}_s \in \mathcal{P}_{C-IRS,s}$ that minimizes the azimuth-elevation-domain area of the reflection beam. This area is calculated as the product of the horizontal and vertical reflection beamwidths in order to serve the subset of under-connected UE positions that was identified by the end of `Step #3)`.
   ➤ Our heuristic differs from related works suggesting the placement of reconfigurable reflectors near the BS or UE to minimize the product-distance path loss [21] in order to instead minimize the loss in bistatic radar cross section (RCS) (with unit m^2) from beam broadening when using a non-reconfigurable IRS such as HELIOS.
5) **Custom-tailoring of HELIOS IRS $\mathcal{H}_s$** to supply $\mathcal{P}_{U-UE,s}$ using an analytical reflection model [19] along with a genetic algorithm (GA) [20] to determine the $2 \cdot M \cdot N$ horizontal and vertical module tilt angles

$(\alpha_{m,n}, \beta_{m,n})$ with $m = 1, \ldots, M$ and $n = 1, \ldots, N$. Our design process is conducted for $M \times N$ shaped IRSs with $M, N = 2, \ldots, 6$, which are suitable for different reflection beamwidths, and $N \geq M$ because we expect broader horizontal than vertical reflection beamwidths. Select the IRS configuration $\mathcal{H}_s$ in terms of $\{N^*, M^*\}$ and $\{\alpha^*_{1,1}, \ldots, \alpha^*_{M^*,N^*}, \beta^*_{1,1}, \ldots, \beta^*_{M^*,N^*}\}$ that maximizes the minimum bistatic RCS in the targeted reflection space.

➤ Considering related works on IRS network planning, the strength of this approach is the co-design of a custom-tailored IRS geometry (exhibiting an optimized reflection beam shape) serving as a complete production blueprint. In contrast, related studies typically assume arbitrarily-sized reconfigurable IRSs with an idealized reflection hull pattern (e.g., [8]) or static IRSs in the form of pole-mounted rotated metal plates with narrow reflection beams [7].

6) **Update the overall connectivity REM** to factor in the reflection by the customized IRS at the identified mounting position [19, 20]:
   a) First sub-channel: Determine the RSRP value (in dBm) of the LOS propagation path from the BS to the IRS by ray-tracing with an isotropic antenna for the IRS.
   b) Second sub-channel: Determine RSRP REM (in dBm) from the IRS position to UE grid via ray-tracing while using the IRS's RCS reflection pattern (in dBsm) as the antenna pattern (in dBi) using 0 dBm transmit power.
   c) Construct IRS-based connectivity REM using the radar equation [19], i.e., by summing up the previous sub-channel RSRPs (in dB) and adding $4\pi/\lambda^2$ (≈ 50.1 dB).
   d) Determine joint connectivity of active and passive components by element-wise max operator between current connectivity REM and IRS REMs from `Step #6c)`.

   ➤ Considering numerous related studies on propagation modeling with IRSs, the strength of this approach is that NLOS propagation paths from the subchannel between the IRS and UE are considered, cf. [7, 8].

   ➤ This is strengthened by employing a realistic 3D IRS reflection pattern with sidelobes, compared to using a ray-tracer with integrated support for engineered EM surfaces (EES) with idealized behavior, i.e., a rectangular reflection lobe without ripples and sidelobes [15].

7) *Return to `Step #2)` for a potential next iteration.*

Against this background, the terminated process yields the following results: *(i)* s describes the required number of IRSs, *(ii)* $\underline{p}_s$ their respective center mounting position in the InF environment, and *(iii)* $\mathcal{H}_s$ contains the HELIOS reflector geometry, yielding a custom-tailored reflection pattern to improve the connectivity of under-connected regions within the service area. Hence, a desired brownfield network planning scheme with entirely passive IRSs components has been presented.

B. Connectivity of mmWave BS with HELIOS IRSs

This section aims to validate the feasibility of the previously proposed planning process by iteratively extending the single BS deployment from Sec. II with passive-static reflectors. This baseline connectivity is shown at the top of Fig. 5, cf. subfigure a), with the left subfigure showing the ambient RSRP distribution on the shop floor and the right side depicting whether the connectivity is sufficient to service the AGVs. As in Sec. II, we reaffirm that the single BS deployment cannot serve the whole service area contained in the production hall, such that at least one IRS is required to serve the highlighted (in red) under-connected UE positions.

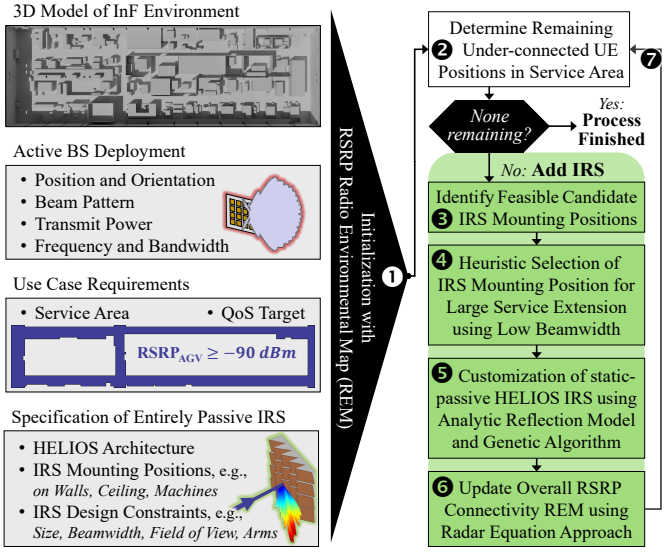

Fig. 4. Overview of proposed planning process: Iterative joint HELIOS IRS placement and custom-configuration at systematically selected candidate position to mitigate under-connected regions in intended service area.

Iterative Deployment Extensions: After the first iteration of our proposed planning process, the previously discussed situation has changed: the first HELIOS reflector has been mounted to the factory hall at the position $\underline{p}_1 = [55.45\,\text{m}, -19.25\,\text{m}, 3.88\,\text{m}]$ with the incident 27.1 GHz wave from the BS impinging from the azimuth angle $\phi_{in} = -11.02°$ and elevation angle $\theta_{in} = 1.29°$. Closeness to the previously considered second BS position confirms the validity of this position. Whereas this position has LOS to all under-connected UE positions, our scheme adheres to the 20° beamwidth IRS design constraint and thus targets the 15.94° broad azimuth reflection range $\phi_{out} \in [-87.17°, -71.23°]$ and the 13.43° broad elevation-plane reflection range $\theta_{out} \in [-22.60°, -9.17°]$ to maximize the gain in the service area. Using a reflection model-based HELIOS design process with a metaheuristic (here: GA), a 4×5 HELIOS reflector is custom-tailored within 9 min 44 s (239 GA generations, 25,692 RCS pattern calculations), thereby attaining a peak gain of 16.65 dBsm in the above-described angular reflection space. Its impact can be clearly seen in Fig. 5 b), with high gains in RSRP in the right corridor at $x \approx 55\,\text{m}$, upon which we focus with help of a 3D-printed model at a scale of 1:200 in Fig. 6. Accordingly, it can be clearly observed that previously under-connected UE positions are now served with sufficient signal strength for the AGV services (RSRP $\geq -90\,\text{dBm}$).

The remaining under-connected regions are addressed

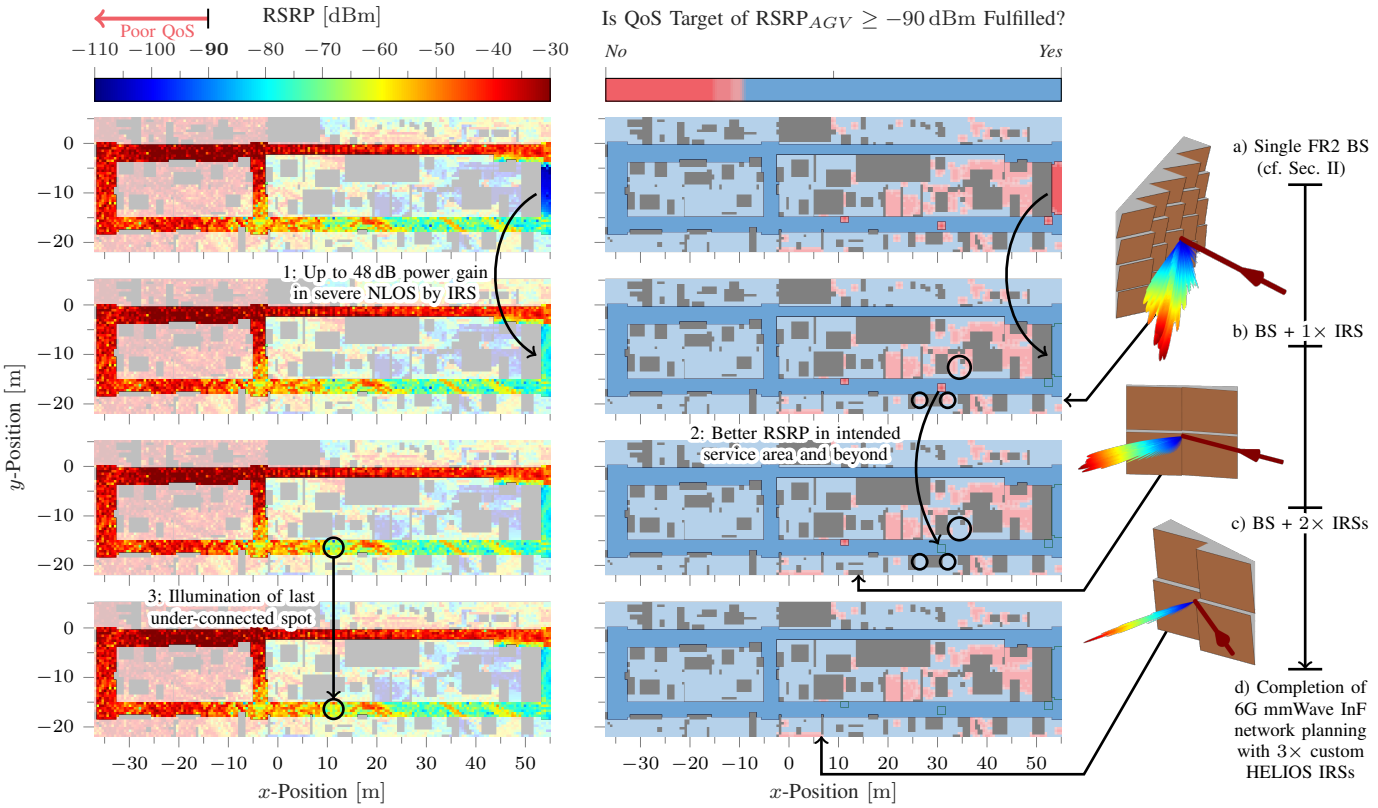

Fig. 5. Improvement of mmWave connectivity in under-connected regions of the indoor factory environment compared to *(a)* single BS deployment: *(b)* After first iteration, introduced HELIOS IRS serves NLOS corridor. *(d)* Deployment of third custom-tailored IRSs realizes QoS-compliant coverage on shop floor.

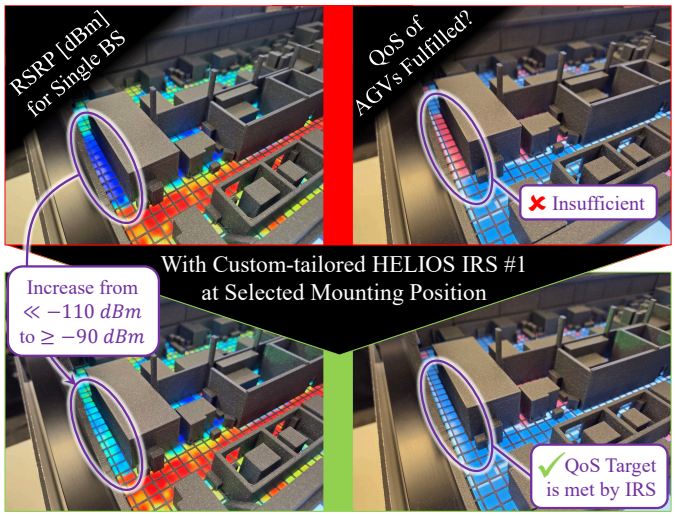

Fig. 6. Showcasing potential of HELIOS IRS for large-scale expansion of mmWave service area: Connectivity REMs *(top)* before and *(bottom)* after deployment of the first IRS depicted in context of a scaled 3D-printed model.

in the subsequent iterations: The second HELIOS IRS is attached to another wall of the InF hall with position $\underline{p}_2 = [14.05\,\mathrm{m}, -23.23\,\mathrm{m}, 5.00\,\mathrm{m}]$ with the BS's radiated signal impinging from the azimuth angle $\phi_{in} = 66.77°$ and elevation angle $\theta_{in} = 1.03°$. A 2×2 HELIOS IRS geometry with a peak RCS of 20.36 dBsm, identified in 27,565 RCS pattern calculations, is employed to serve the reflection space 10.37° broad azimuth reflection range $\phi_{out} \in [-78.69°, -68.32°]$ and the 5.89° broad elevation-domain reflection range $\theta_{out} \in [-11.02°, -5.13°]$. Once again, additional under-connected UE positions could be covered from this position, however, the beamwidth constraint was successfully enforced. Fig. 5 c) shows that the connectivity blackspot in the vicinity of the position $(30\,\mathrm{m}, -15\,\mathrm{m}, 1.5\,\mathrm{m})$ is successfully illuminated. Beyond the intended local connectivity improvement, a positive impact on positions outside the targeted service area can also be observed, for example, from reflection sidelobes and object reflections, cf. region at $x \approx 35\,\mathrm{m}$ and $y \approx -10\,\mathrm{m}$ as well as the region at x-coordinates 25 m to 35 m with y-coordinate of approximately −20 m.

The third and final iteration illuminates the remaining under-connected spot in the service area at the position $[11.25\,\mathrm{m}, -15.09\,\mathrm{m}, 1.5\,\mathrm{m}]$. HELIOS IRS #3 is placed at position $\underline{p}_3 = [6.55\,\mathrm{m}, -23.23\,\mathrm{m}, 4.0\,\mathrm{m}]$. It was customized within 22,810 steps and reflects the incident signal from direction $\phi_{in} = 63.32°, \theta_{in} = 2.33°$ into direction $\phi_{out} = -30.01°, \theta_{out} = -14.90°$. Against this background, the configuration process selects a 2×2 module layout with the optimal surface tilt alignment realizing a peak gain of 32.12 dBsm. Fig. 5 d) shows that the RSRP throughout the targeted service area for the mobile AGVs has now reached the requirement of –90 dBm at all positions. Similar to regular network planning for active BSs, the process is therefore successfully terminated after placing the least amount of fully passive communication infrastructure while guaranteeing the required service level on the shop floor [16].

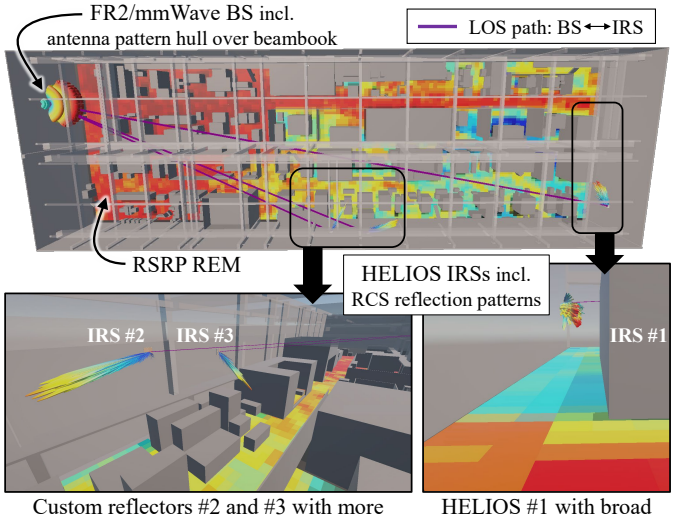

Fig. 7. Overall result of proposed brownfield network planning solution is showcased via VR view of complex production environment along with horizontal-plane RSRP REM and 3D IRS models including reflection pattern.

Final Network Setup: The overall attained mmWave network deployment consisting of one BS and three HELIOS IRSs is provided by a VR-based twin of the 6G InF environment in Fig. 7. Therein, the three reflectors have yielded power gains of up to 47.98 dB within the production hall, and the connectivity was improved at 4.29 % of the considered UE positions. Importantly, when compared to Sec. II, *we showed that, without a loss in performance, future 6G networks may use fewer high-power BSs by switching to entirely passive IRSs that are custom-tailored to the deployment scenario.* Thus, the more sustainble network design consumes less power, i.e., hundreds of Watts per saved BS, while also reducing infrastructure investment and operational costs for the operator [17, Ch. 6.5.2].

IV. Conclusions and Outlook

This work has demonstrated a computational network planning approach for future IRS-enhanced 6G communications in complex industrial environments. The connectivity goals of AGVs were met efficiently by adding three IRSs at strategic positions yielding tens of dB power gain, thereby mitigating the need for an additional full-blown active mmWave BS. Moreover, to the best of our knowledge, this contribution is the first work that includes a custom-tailoring process for entirely passive HELIOS IRSs with static reflection patterns.

In future works, we will extend and benchmark the utilized HELIOS reflector design process to also facilitate dynamically-sized IRSs providing reflection patterns with predetermined in-beam gains. Our ongoing research aims to integrate a machine learning-based propagation model to mitigate the manual steps in the context of ray-tracing simulations while drastically reducing the computing time [22]. We are also investigating the implications of preset limitations, such as the IRS field of view, on the planning results in different radio environments in terms of outline, clutter, and BS positions.

Acknowledgment

This work was funded by the German Federal Ministry of Research, Technology and Space (BMFTR) in the course of the *6GEM* research hub under grant 16KISK038 and the *PANGOLIN Networks* project under grant 16KIS2357. The authors thank the Fraunhofer IPT for access to the shop floor model, as well as Marco Danger, Robin Becker, and David Ronschka for supporting the production of the immersive scaled 3D model- and VR-based demonstrators.

References

[1] Orange SA. (2021, Jul.) 5G explores 26 GHz band. [Online]. Available: https://hellofuture.orange.com/5g-explores-26-ghz-band (Accessed 2025-07-25).
[2] B. Sihlbom, M. I. Poulakis, and M. Di Renzo, "Reconfigurable intelligent surfaces: Performance assessment through a system-level simulator," *IEEE Wirel. Commun.*, vol. 30, no. 4, pp. 98–106, Aug. 2023.
[3] S. Häger, M. Kaudewitz, F. Schmickmann, S. Böcker, and C. Wietfeld, "Field performance evaluation of a mechatronic reflector system in a private mmWave network environment," *IEEE Open J. Commun. Soc.*, vol. 6, pp. 5005–5029, Jun. 2025.
[4] A. Schott, A. Ichkov, N. Beckmann, N. König, and L. Simić, "Mm-Wave connectivity in industrial environments: A measurement study at 28 and 60 GHz," in *Proc. IEEE GLOBECOM Conf.*, Dec. 2024.
[5] A. Ramírez-Arroyo *et al.*, "FR2 5G networks for industrial scenarios: Experimental characterization and beam management procedures in operational conditions," *IEEE Trans. Veh. Technol.*, vol. 73, no. 9, pp. 13 513–13 525, Sep. 2024.
[6] M. Danger, C. Arendt, H. Schippers, S. Böcker, N. Beckmann, R. Schmitt, and C. Wietfeld, "6G industrial networks: Mobility-centric evaluation of multi-cell mmWave systems," in *Proc. IEEE VTC-Spring Conf.*, Jun. 2025.
[7] C. K. Anjinappa, F. Erden, and I. Güvenç, "Base station and passive reflectors placement for urban mmWave networks," *IEEE Trans. Veh. Technol.*, vol. 70, no. 4, pp. 3525–3539, Apr. 2021.
[8] E. Tohidi *et al.*, "Near-optimal LOS and orientation aware intelligent reflecting surface placement," in *Proc. IEEE ICC Conf.*, May 2023.
[9] G. Encinas-Lago *et al.*, "A cost-effective RISs deployment to abate the coverage problem in B5G networks," *IEEE Trans. Wirel. Commun.*, vol. 23, no. 10, pp. 15 276–15 290, Oct. 2024.
[10] Fraunhofer Institute for Production Technology (Fraunhofer IPT). (2022, Jul.) 5G-industry campus Europe. DOI: 10.24406/publica-55.
[11] 3GPP, "TSG RAN; study on channel model for frequencies from 0.5 to 100 GHz (release 19)," Technical Report (TR) 38.901, Jun. 2025.
[12] I. F. Priyanta *et al.*, "Towards 6G-driven digital continuum in logistics," *Logistics Journal: Proceedings*, no. 19, pp. 1–12, Oct. 2023.
[13] O-RAN Alliance, "O-RAN WG next generation research group; use case analysis on mmWave antenna distribution (mWAD)," Research Report, Jul. 2024, version 2.00, release 003.
[14] M. Danger, C. Arendt, H. Schippers, S. Böcker, M. Mühleisen, P. Becker, J. B. Caro, G. Gjorgjievska, M. A. Latif, J. Ansari, N. Beckmann, N. König, R. Schmitt, and C. Wietfeld, "Performance evaluation of IRS-enhanced mmWave connectivity for 6G industrial networks," in *Proc. IEEE M&N Symp.*, Jul. 2024, best paper young author award.
[15] Remcom, Inc. Wireless InSite propagation software. [Online]. Available: https://www.remcom.com/wireless-insite (Accessed 2025-05-24).
[16] M. Geis, C. Bektas, S. Böcker, and C. Wietfeld, "AI-driven planning of private networks for shared operator models," in *Proc. IEEE LANMAN Symp.*, Jul. 2024.
[17] O-RAN Alliance, "O-RAN WG use cases and overall architecture; network energy saving use cases," Technical Report, Jun. 2023, version 2.00, release 003.
[18] Fraunhofer IIS, "6G energy efficiency and sustainability," White Paper, Jan. 2023, version 1.0. [Online]. Available: https://www.iis.fraunhofer.de/content/dam/iis/en/doc/lv/Whitepaper6GSustainability.pdf (Accessed 2025-07-02).
[19] S. Häger, S. Böcker, and C. Wietfeld, "Reflection modeling of modular passive IRS geometries," *IEEE Wirel. Commun. Lett.*, vol. 14, no. 5, pp. 1366–1370, May 2025.
[20] S. Häger, M. Danger, K. Heimann, Y. Gümüs, S. Böcker, and C. Wietfeld, "Custom design and experimental evaluation of passive reflectors for mmWave private networks," in *Proc. IEEE LANMAN Symp.*, Jul. 2024, best paper award.
[21] Q. Wu, S. Zhang, B. Zheng, C. You, and R. Zhang, "Intelligent reflecting surface-aided wireless communications: A tutorial," *IEEE Trans. Commun.*, vol. 69, no. 5, pp. 3313–3351, May 2021.
[22] M. Geis, S. Häger, and C. Wietfeld, "Taming mmWave connectivity prediction with DRaGon: AI propagation modeling for cluttered industrial environments," in *Proc. IEEE FNWF Conf.*, Nov. 2025.